Part 4. Circumstellar Envelopes

https://doi.org/10.1017/S0074180900203215 Published online by Cambridge University Press

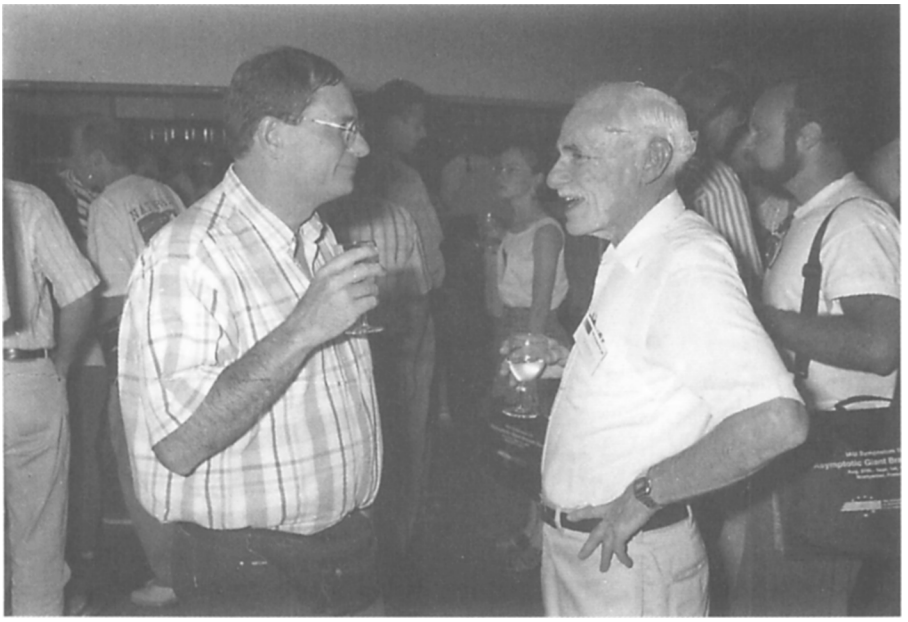

Alfred Glassgold and Robert Lucas probing organic molecules

https://doi.org/10.1017/S0074180900203215 Published online by Cambridge University Press

Asymptotic Giant Branch Stars
T. Le Bertre, A. Lèbre and C. Waelkens, eds.
I.A.U. Symposium 191, 1999

Millimeter-wave Interferometry of Circumstellar Envelopes

Robert Lucas and Michel Guélin
Institut de RadioAstronomie Millimétrique, 300, rue de la Piscine, 38406 Saint Martin d'Hères, France

Abstract. We present some of the most significant results obtained in the last few years with the IRAM Plateau de Bure interferometer and with other instruments on the detailed mapping of circumstellar envelopes.

1. Introduction

In the last few years millimeter-wave observations of circumstellar envelopes have considerably improved in both angular resolution and sensitivity. This is due to progress in receiver technology, to the increasing collecting area available at all millimeter-wave interferometers, and to the possibility to use these instruments down to 1mm wavelength. Sub-arcsecond resolution maps may now be obtained for many objects. The spectacular images contain information on the detailed morphology of expanding circumstellar envelopes, both for standard AGB stars and more evolved proto-planetary envelopes; they allow to conduct studies on the chemistry in the innermost region of the outflows, as well as to map the remnants of old high mass-loss episodes.

The millimeter-wave interferometers currently in operation are Berkeley Illinois Maryland Array and the Owens Valley Radio Observatory (both in California, USA), the Nobeyama Millimeter Array (Nobeyama, Japan), and the Plateau de Bure Interferometer of IRAM (France). They operate in the 3 mm (80-115 GHz) and 1.3 mm (210-250 GHz) windows, and reach typical resolutions of $\sim 2''$ (at 3 mm) or $0.5''$ (at 1.3 mm), with fields of view of 20-120″, which may be extended by combining several fields (mosaics).

2. A CO survey of circumstellar envelopes

A CO survey of circumstellar envelopes has been undertaken at the Plateau de Bure interferometer by Neri et al. (1998). Forty-six AGB and post-AGB stars were mapped in the CO J=1–0 line in the snapshot mode. The IRAM 30 m telescope was used to obtain the J=1–0 short spacings and CO J=2–1 maps. The derived properties include positions (with an accuracy of $0.5''$), fluxes, and radii using both model fits to the visibilities and single dish maps. Crude interferometer maps are also presented, despite the limited *uv* coverage. The observed line shapes are mostly characteristic of thick envelopes, while some objects may be two-component (detached) shells. The morphology, size and asymmetries were analysed. Most envelopes have a spherical appearance ($\sim 70\%$), but some shells

present a significant asymmetry (RS Cnc, M1-92, R Cas), with a pronounced bipolar kinematical signature. Mass loss rates and ^{12}CO photodissociation radii are calculated for 38 stars, using the method of Loup et al. (1993). An empirical relation is found between the ^{12}CO photodissociation radii and the observed radii, indicating that the CO extents are limited by photodissociation by interstellar UV radiation.

3. Observations of IRC +10216

IRC +10216 (CW Leo) is the nearest carbon star; its distance is of the order of 150 pc. It has a massive envelope (mass loss rate $\sim 2\ 10^{-5}\ M_\odot$), expanding at 14.5 km/s. The stellar radius is $R_* \sim 7\ 10^{13}$ cm. The optical nebula is elongated along a position angle of 20°. In the inner envelope, one detects photospheric species, affected by neutral reactions and interaction with dust in the zone of dust formation and acceleration. The outer envelope extends in CO out to 200″ radius. It has a rich carbon chemistry, with about 50 different molecules detected out to 30″ radius, which appears dominated by photodissociation and reactions with photodissociation products, as well as, possibly, photodesorption from dust grains (see the review by Glassgold in this volume).

3.1. The inner envelope

Continuum emission at millimeter wavelengths The continuum emission of IRC +10216 is easily detected with the IRAM interferometer at 3 mm wavelength (Lucas & Guilloteau 1992) and at 1.3 mm (Lucas 1997). At the highest frequencies the source emission may be split into a point source and extended emission (Lucas et al., in preparation). Table 1 gives a summary of the source properties.

Table 1. IRC +10216 continuum emission at millimeter wavelengths

Frequency (GHz)	Point source (mJy)	Extended emission (mJy)	size (″)
89.	65 ± 1	8 ± 1	2.4 ± 0.1
216.	316 ± 2	178 ± 5	1.3 ± 0.1
235.	407 ± 6	280 ± 42	1.8 ± 0.4
242.	486 ± 7	270 ± 22	1.6 ± 0.3

The point source is identified to the photospheric emission, while the extended part is due to thermal emission from dust in the inner envelope. Groenewegen et al. (1997) have observed the continuum emission at 1 mm using a bolometer at the 30-m telescope. They find a peak flux of 0.7 Jy, after subtracting a contribution of similar magnitude due to line contamination in the bolometer passband. The integrated single dish flux in the primary beam of the 15m Plateau de Bure antennas, estimated from the bolometer map, is 1.6 Jy,

which could mean, if the line contamination in the 30m data has been correctly estimated, that half of the emission from dust is resolved out at PdBI.

Vibrationally excited lines Vibrationally excited rotational lines of SiS and CS may be used to investigate the inner envelope of IRC+10216: their lower levels lie in energy about 10^3K above the ground state, and thus they can only be excited at a few stellar radii from the star in the presence of a high enough kinetic temperature or of a strong IR field. We have observed the $v = 1, J = 13 - 11$ transition of SiS and the $v = 1, J = 5 - 4$ transition of CS in IRC+10216, with the Plateau de Bure interferometer. Both transitions are in the 1.3 mmwindow, where the available resolution can reach $0.5''$ in the most extended configuration.

Both emissions are spatially resolved, and no departure from spherical symmetry is seen (Fig. 1). The source size, derived by a Gaussian fit to the visibilities, is $\sim 0.35''$ or 7 10^{14}cm, which represents $\sim$ 10 stellar radii, for both lines. The brightness temperatures are 1200 K for SiS and 900 K for CS, which means that both lines are close to be optically thick, given the kinetic temperatures expected at a few stellar radii (1000-1500 K). We have tentatively modelled the SiS emission, using source model parameters from Groenewegen (1997); the rotational emission from SiS in the excited vibrational state is due to collisional and radiative excitations (the source size at $\lambda = 10\mu$m is $0.9''$ in diameter); the emerging line profile and the spatial distribution are well reproduced with an abundance of SiS decreasing from 10^{-5} at 3 stellar radii to 7×10^{-6} at 12 stellar radii, in agreement with infrared absorption measurements (Boyle et al. 1994). The predicted size of the SiS $v = 1$ emission is mainly determined by the size of the 10 μm emitting region. We thus mainly check that the dust forming region actually coincides with the region where the AGB wind is accelerated. Measurements of this kind at higher angular resolution should in the next decade or so provide detailed information on the kinematics of this important part of the circumstellar envelope. Radiative transitions within the lowest bending states of HC_3N, C_3H, C_4H and MgNC, a few 10^2 K high in energy, are also detected at $12''$ radius.

Ground state lines The emission in the inner envelope is dominated by lines of CO, HCN, SiO, CS, SiS, SiC_2, etc. Some of their lines have been mapped with interferometers by Bieging et al. (1984), Bieging & Nguyen-Q-Rieu (1989), Bieging & Tafalla (1993), Dayal & Bieging (1995), Gensheimer et al. (1995); maps of SiS, SiC_2, CS have been presented by Lucas et al. (1995). Those maps lack the sub-arcsecond resolution needed to study the inner shell.

Recent, unpublished CO $J = 2 - 1$ observations at Plateau de Bure show no obvious departure from spherical symmetry at angular radii larger than $\sim 2''$. On the opposite, maps of SiS ($J = 12 - 11$) at 217 GHz show enhanced emission in the southern half on the envelope; apparently two inner shells are present at radii $\sim 4''$ and $\sim 8''$. They are also seen in AlF emission.

3.2. The outer envelope

Many maps have been made, using the Hat Creek interferometer (Bieging et al. 1984; Bieging & Nguyen-Q-Rieu 1988, 1989; Bieging & Tafalla 1993; Dayal & Bieging 1993, 1995; Gensheimer et al. 1995), which support a chemistry

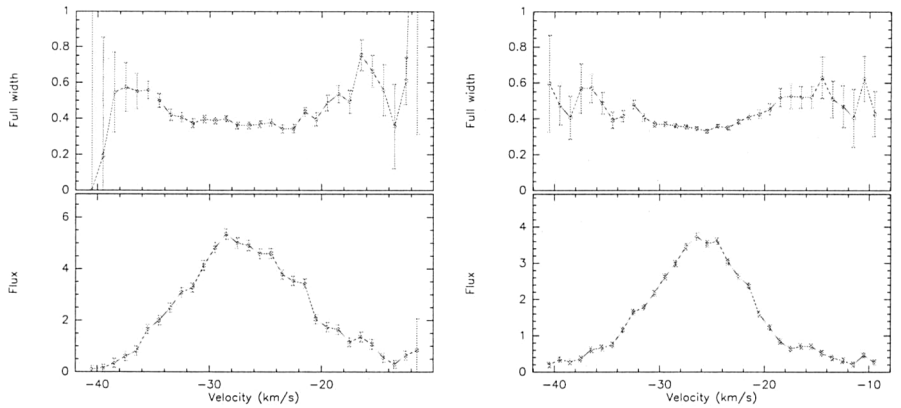

Figure 1. SiS $v = 1, J = 13 - 11$ (left) and CS $v = 1, J = 5 - 4$ (right) emission profiles from IRC +10216. We have plotted the result of Gaussian source model fits to the visibilities: the upper boxes give the size at half-power, in arcseconds, and the lower boxes the integrated fluxes in Jy.

based on photochemical and radical reactions (see the review by Glassgold in this volume). More detailed maps are now available from the Plateau de Bure interferometer (Guélin et al. 1993a, 1993b, 1996; Lucas et al. 1995). They are obtained at better angular resolution (3″) and give more insights on the detailed structure of the outer envelope. More species are mapped, resulting from the HCN chemistry (HCN, CN, HNC, C_3N, $HC^{13}CCN$, HC_5N), from the C_2H_2 chemistry (C_2H, C_3H, C_4H, C_6H), but also species containing metals, like NaCl, NaCN, AlF, MgNC (Guélin et al. 1993a). A recent map of the ion HCO^+ is shown in Fig. 2 (see Glassgold's review for a discussion of this result).

A comparison of the spatial distributions of four species is given in Fig. 3. Both HNC and HC_3N are less extended than CN; emissions of similar products with different number of carbon atoms tend to be coincident, e.g. C_3H and C_4H, or HC_5N and HC_3N. The latter is not really expected from current theory, where chains are built step by step through gas phase reactions, which would predict a larger radial extent for the longer carbon chains. In fact these models are assuming constant and isotropic mass loss, while the maps show considerable structure, both radially and azimuthally, in most species. For instance the CN and HNC emissions show clearly a double shell structure, especially in the NW region.

In Fig. 4 we have plotted the location of the emission maxima ('clumps') in all maps obtained so far. A general picture emerges where a series of concentric shells are present, at approximate radii of 4, 8, 15, and 25″. The shell at 15″ is the one where the the largest number of different species are found; it appears smaller in CS and SiC_2 than in HNC and CN. At this point it is not yet clear if we are seeing substructure in this shell or only chemical segregation.

https://doi.org/10.1017/S0074180900203215 Published online by Cambridge University Press

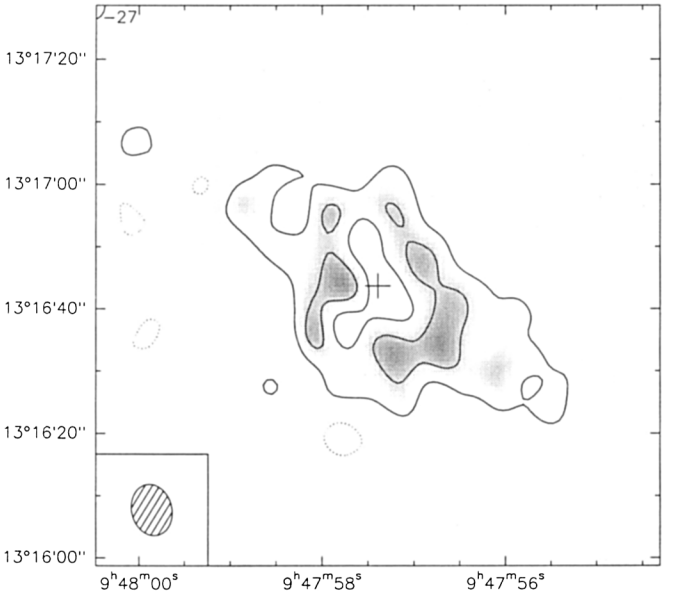

Figure 2. The IRC+10216 emission of HCO^+ mapped with the Plateau de Bure interferometer. The central 10 km/s of the emission profile are integrated. This is a very weak line: the contour spacing is 5 mJy/beam.

4. Detached envelopes

The rate at which AGB stars lose mass is known to evolve with time, very probably both on long time scales and on short time scales. Thermal pulses and mechanical oscillations are believed to modulate on short time scales. The most direct indications for actual changes of mass loss rates came from the detection of geometrically thin CO shells around a few carbon stars: R Scl, U Ant, S Sct, and TT Cyg (Olofsson et al. 1990, 1996). Two other carbon stars have large, detached dust shells (Waters et al. 1994; Izumiura et al. 1996). The CO shells contain a few hundredths of a solar mass. The shell widths, however, cannot be resolved by single dish observations. Only two such objects have been so far studied with interferometers, U Cam and TT Cyg.

The shell around U Cam was observed in HCN and CN at Plateau de Bure by Lindqvist et al. (1996). They separated an outer extended shell of radius 7 10^{16}cm, expanding at 25 km/s, and an inner envelope, of radius 6 10^{15}cm, expanding at 13 km/s. A preliminary ^{12}CO $J = 2 - 1$ map by Linqvist et al. (in prep.) was obtained at Plateau de Bure, which unambiguously shows the detached nature of the outer shell.

The shell around TT Cyg was partially mapped in ^{12}CO $J = 1 - 0$ and $2 - 1$ by Olofsson et al. (1996, 1998). They found a remarkably thin shell of CO gas (radius 34″, thickness 1.3″), containing 0.02 solar masses of gas. The shell shows only small deviations from spherical symmetry. Mass loss is currently occurring

https://doi.org/10.1017/S0074180900203215 Published online by Cambridge University Press

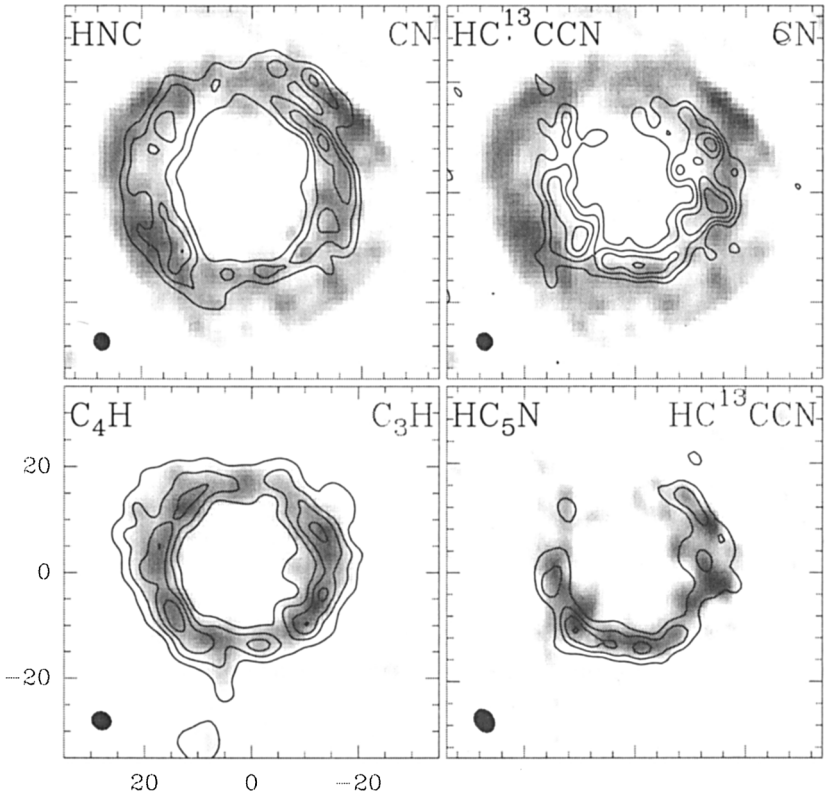

Figure 3. Comparison of the extents of various molecular emissions in the outer envelope of IRC +10216. All plots represent the emission at the systemic velocity (-27 km/s) and are at the same angular scale. Grey scale correspond to the species noted in the upper right corners, contours to those noted in the upper left. Except for CN, no correction has been made for primary beam attenuation. Beam widths are drawn in the lower left corner of each box.

at a rate of $\sim 10^{-8}$ $M_\odot$/yr. A preliminary map of the complete shell is shown in Fig. 5.

5. The multiple molecular jets in AFGL 2688

AFGL 2688, the Egg Nebula, is one of the few objects in the transition phase from the AGB to the planetary nebula phase. It left the AGB about a hundred years ago. Its optical appearance in the visible and in the infrared continuum is that of a bipolar nebula (Sahai et al. 1998a, 1998b), scattering the light of the cool central star, which is surrounded by a cold and dense circumstellar envelope shocked by a warm fast wind (Young et al. 1992). Observations of H_2 in the near-infrared have revealed that high velocity gas is also present in the east-west

https://doi.org/10.1017/S0074180900203215 Published online by Cambridge University Press

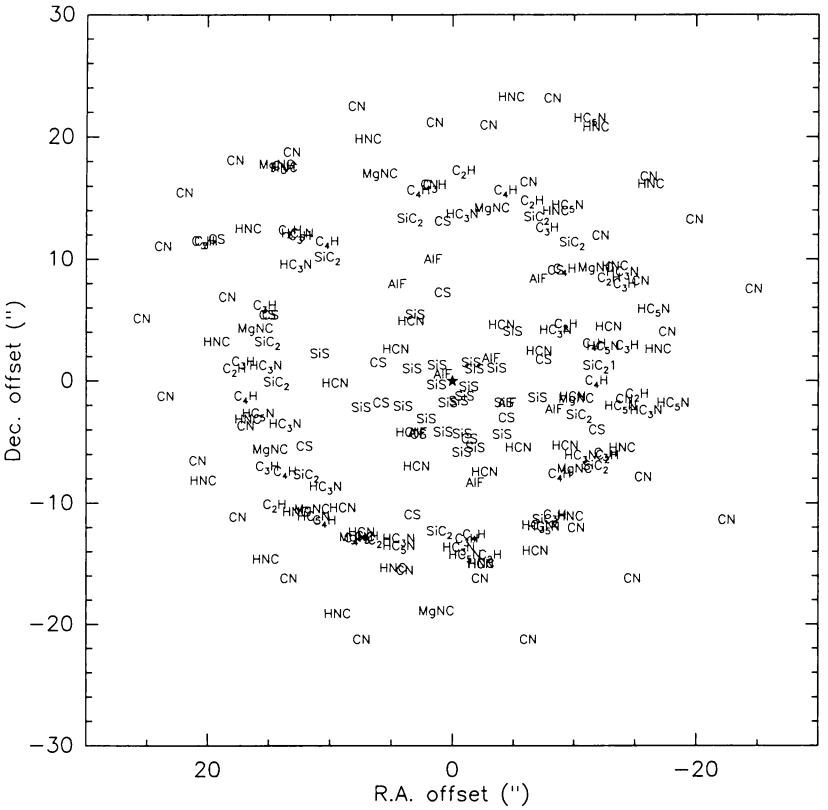

Figure 4. The location of clumps in the IRC +10216 envelope. The relative maxima in the emission map of each species are plotted on the same map and labelled with the name of the molecule.

direction, suggesting a quadrupolar outflow (e.g.: Cox et al. 1997; Sahai et al. 1998b).

Previous interferometric images in the molecular lines (Yamamura et al. 1995; Bieging & Nguyen-Q-Rieu 1996; Kasuga et al. 1997) lacked the resolution to investigate the detailed kinematics of this source. We have made ^{12}CO $J = 2 - 1$ observations of this source at Plateau de Bure (Cox et al., in preparation), with an angular resolution of $1.0 \times 1.6''$. Four outflows are observed, which are obviously linked to the four H_2 emission regions, and a strong 1 mm continuum (peak flux 200 mJy/beam) is coincident with the obscuring dust in the IR maps (Fig. 6).

6. Prospects

On the long term, considerable progress in this field is expected from the availability of a new generation of interferometers during the next decade. Large arrays are being planned, such as the MMA in the US, the LSA in Europe,

https://doi.org/10.1017/S0074180900203215 Published online by Cambridge University Press

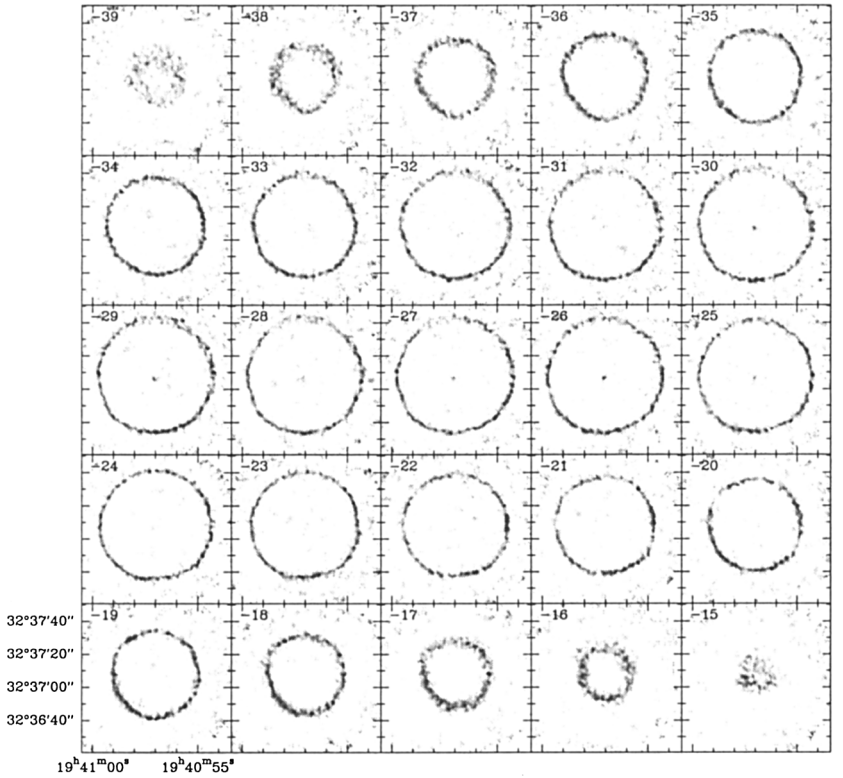

Figure 5. TT Cyg ^{12}CO $J = 1 - 0$ emission from Olofsson et al. (in preparation). The channel maps are labelled by their LSR velocity in km/s.

the LMSA in Japan. It is expected that at least two of these projects will be merged into a single, even more powerful instrument. Collecting areas of several thousand square meters are foreseen. Those instruments should reach $\sim 0.1''$ resolutions, enabling much more detailed studies of the prototypal objects, down to a few stellar radii, and to investigate the problems of dust formation and wind acceleration. The frequency coverages will be extended to the sub-millimeter range, where dust emission is stronger, and other chemical species (hydrides) may be observed. The ten-fold improved sensitivity will enable to map circumstellar envelopes of AGB stars up to the center of the Galaxy.

References

Bieging J.H., Chapman B., Welch W.J., 1984, ApJ 285, 656
Bieging J.H., Nguyen-Q-Rieu, 1989, ApJ 343, L25
Bieging J.H., Nguyen-Q-Rieu, 1996, AJ 112, 706
Bieging J.H., Nguyen-Q-Rieu, 1988, ApJ 329, L107

https://doi.org/10.1017/S0074180900203215 Published online by Cambridge University Press

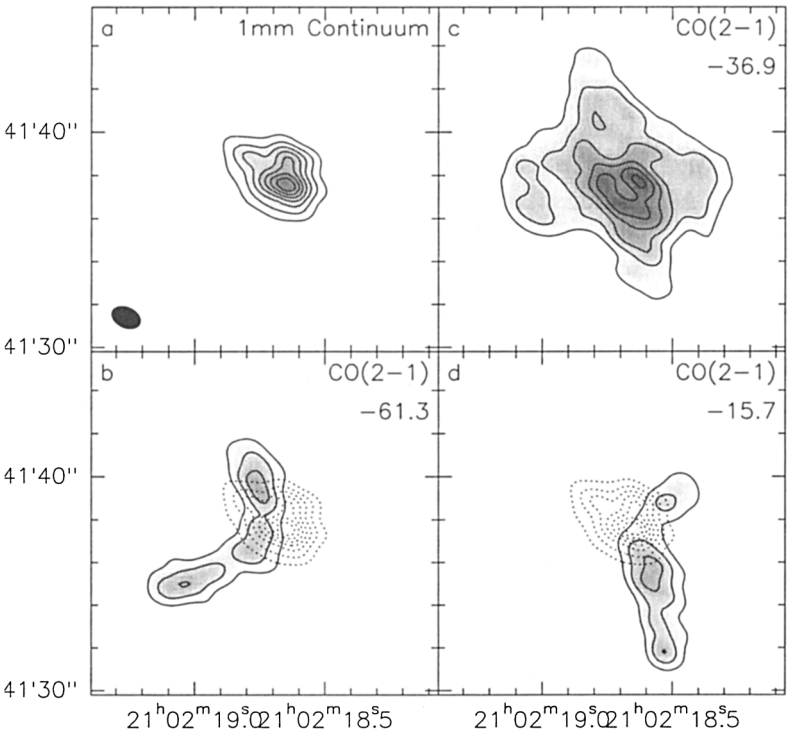

Figure 6. AFGL 2688: CO emission in the central channel; CO emission in two outer channels overlaid with the H_2 emission.

Bieging J.H., Tafalla M., 1993, AJ 105, 576

Boyle R.J., Keady J.J., Jennings D.E., Hirsch K.L., Wiedemann G.R., 1994, ApJ 420, 863

Cox P., Maillard J.-P., Huggins P., Forveille T., Simons D., Guilloteau S., Rigaut F., Bachiller R., Omont A., 1997, A&A 321, 907

Dayal A., Bieging J.H., 1993, ApJ 407, L37

Dayal A., Bieging J.H., 1995, ApJ 439, 996

Gensheimer P.D., Likkel L., Snyder L.E., 1995, ApJ 439, 445

Groenewegen M.A.T., 1997, A&A 317, 503

Groenewegen M.A.T., van der Veen W.E.C.J., Lefloch B., Omont A., 1997, A&A 322, L21

Guélin M., Lucas R., Cernicharo J., 1993a, A&A 280, L19

Guélin M., Lucas R., Neri R., 1993b, in *34th Herstmonceux Conference*, ed. R. Clegg, Cambridge

Guélin M., Lucas R., Neri R., 1996, in Science with large millimeter arrays, P.A. Shaver (ed.), Springer, p. 276

Izumiura H., Hashimoto O., Kawara K., Yamamura I., Waters L.B.F.M., 1996, A&A 315, L221

https://doi.org/10.1017/S0074180900203215 Published online by Cambridge University Press

Kasuga T., Yamamura I., Deguchi S., 1997, A&A 320, 575

Lindqvist M., Lucas R., Olofsson H., Omont A., Eriksson K., Gustafsson B., 1996, A&A 305, L57

Loup C., Forveille T., Omont A., Paul J.F., 1993, A&AS 99, 291

Lucas R., 1997, Ap&SS 251, 247

Lucas R., Guélin M., Kahane C., Audinos P., Cernicharo J., 1995, Ap&SS 224, 293

Lucas R., Guilloteau S., 1992, A&A 259, L23

Neri R., Kahane C., Lucas R., Bujarrabal V., Loup C., 1998, A&AS 130, 1

Olofsson H., Bergman P., Eriksson K., Gustafsson B., 1996, A&A 311, 587

Olofsson H., Bergman P., Lucas R., et al., 1998, A&A 330, L1

Olofsson H., Carlstrom U., Eriksson K., Gustafsson B., Willson L.A., 1990, A&A 230, L13

Sahai R., Hines D.C., Kastner J.H., Weintraub D.A., Trauger J.T., Rieke M.J., Thompson R.I., Schneider G., 1998a, ApJ 492, L163

Sahai R., Trauger J.T., Watson A.M., et al., 1998b, ApJ 493, 301

Waters L.B.F.M., Loup C., Kester D.J.M., Bontekoe T.R., de Jong T., 1994, A&A 281, L1

Yamamura I., Onaka T., Kamijo F., Deguchi S., Ukita N., 1995, ApJ 439, L13

Young K., Serabyn G., Phillips T.G., Knapp G.R., Guesten R., Schulz A., 1992, ApJ 385, 265